Impacts of ultramafic outcrops in Peninsular Malaysia and Sabah on soil and water quality

Mahsa Tashakor, Soroush Modabberi, Antony van der Ent, Guillaume Echevarria

School of Geology, College of Science, University of Tehran, Tehran, Iran

Centre for Mined Land Rehabilitation, Sustainable Minerals Institute, The University of Queensland, Queensland, Australia

Laboratoire Sols et Environnement, Université de Lorraine, INRA, 54000 Nancy, France

Abstract

This study focused on the influence of ultra- mafic terrains on soil and surface water environmental chemistry in Peninsular Malaysia and in the State of Sabah also in Malaysia. The sampling included 27 soils from four isolated outcrops at Cheroh, Bentong, Bukit Rokan, and Petasih from Peninsular Malaysia and sites near Ranau in Sabah. Water samples were also collected from rivers and subsurface waters interacting with the ultramafic bodies in these study sites. Physico-chemical parameters (including pH, EC, CEC) as well as the concentration of major and trace elements were measured in these soils and waters. Geochemical indices (geoaccumulation index, enrichment factor, and concentration factor) were calculated. Al_2O_3 and Fe_2O_3 had relatively high concentrations in the samples. A depletion in MgO, CaO, and Na_2O was observed as a result of leaching in tropical climate, and in relation to weathering and pedogenesis processes. Chromium, Ni, and Co were enriched and confirmed by the significant values obtain- ed for Igeo, EF, and CF, which correspond to the extreme levels of contamination for Cr and high to moderate levels of contamination for Ni and Co. The concentrations of Cr, Ni, and Co in surface waters did not reflect the local geochemistry and were within the permissible ranges according to WHO and INWQS standards. Subsurface waters were strongly enriched by these elements and exceeded these standards. The association between Cr and Ni was confirmed by factor analysis. The unexpected enrichment of Cu in an isolated component can be explained by localized mineralization in Sabah.

Introduction

Ultramafic rocks are composed of ferromagnesian-rich minerals assigned to ophiolite suites, which have been produced from the hydrothermal alteration of peridotites along tectonic convergent plate margins (Coleman and Jove 1992; O'Hanley 1996; Alexander et al. 2006). Ultramafic rocks and derived soils present an elevated geochemical background notably for chromium (Cr), cobalt (Co), and nickel (Ni) (Schwertmann and Latham 1986; Brooks 1987; Kierczak et al. 2007, b; Massoura et al. 2006; Hseu et al. 2007, 2015; Cheng et al. 2009; Quantin et al. 2008; Tashakor et al. 2014). Ultramafic rocks can be metamorphically altered to serpentinites, which consist of serpentine group minerals (such as antigorite, lizardite, and chrysotile) in addition to resistant and/or unaltered minerals (such as chromite) of the ophiolite suites. Weathering is more intensive in humid tropical and subtropical environments. Tropical climates are characterized by high humidity and temperature throughout the year which lead to complete and prolonged weathering and formation of deep lateritized soils (Ferralsols). Pedogenic processes and the type of soil produced during the weathering process depends largely on the climatic conditions (Brooks 1983) and for this reason ultramafic soils in Southeast Asia differ significantly from those in Iran, Oman, Turkey, and Greece (Hseu and Iizuka 2013; Galey et al. 2017; Kierczak et al. 2007, b; Vithanage et al. 2014; Alexander and DuShey 2011; Georgopoulos et al. 2018). Soils developed from ultramafic rock are sources of natural geogenic contamination, which has the potential to adversely affect environment and human health (Oze et al. 2004; Hseu et al. 2006; Hseu et al. 2016; Kierczak et al. 2008; Kumar and Maiti 2013).

In most soils, Cr and Ni are < 100 mg kg^{-1} (Kabata-Pendias and Mukherjee 2007), but in ultramafic soils the concentrations of these elements can reach up to 125,000 and 10,000 mg kg^{-1}, respectively (Shanker et al. 2005; Hseu 2006). The world average content of soil Co is 4.5– 12 mg kg^{-1}, but in ultramafic soils Co can reach up to 200 mg kg^{-1} (Kabata-Pendias and Mukherjee 2007). In addition to trace metal toxicity, ultramafic soil exerts challenging conditions for plants due to deficiencies in essential plant mineral nutrients (phosphorus; P, potassium; K), excess of magnesium (Mg), and an imbalance of magnesium to calcium (Ca) (Ca/Mg < 1) (van der Ent 2011; 2017), which can lead to stunted growth and physiognomic alterations in plant species growing on these soils (Brooks 1987; Boyd et al. 2004, 2009).

Recent estimates suggest that over 3 billion people worldwide experience deleterious effects through deficiency or toxicity range of trace elements (Kabata- Pendias and Mukherjee 2007). Consequently, soil quality issues are becoming a global environmental concern (Ashraf et al. 2015). The geochemical anomalies of ultramafic soils may lead to risks of elemental transfer to surrounding waters and runoff and ground waters draining ultramafic terrains can be charged with potentially toxic elements (Rahim et al. 1996; Vardaki and Kelepertsis 1999; Kar et al. 2008). Water contamination in areas characterized by mineral-bearing soil formations are known to cause serious water contamination in some places (Yuen 1996; Voutsis et al. 2015; Shah et al. 2012). However, physico-chemical characteristics of the soil and stream water, as well as the mineralogy of parent materials, can also play an inhibiting role on releasing and leaching elements (Wesolowski 2003). In Malaysia, several ultramafic formations occur, including some of the world's largest ultramafic outcrops in the Malaysian State of Sabah on the Island of Borneo (Van der Ent et al. 2013), as well as minor ultramafic outcrops in Peninsular Malaysia. Despite their interesting characteristics, these ultramafic outcrops have remained relatively unexplored from an environmental point of view (van der Ent et al. 2018). It is hypothesized that naturally metal-loaded ultramafic bedrocks under tropical climatic conditions are rapidly disintegrated and release potentially harmful trace elements, which may subsequently ingress to agricultural land and into sur- face water used for human consumption. Therefore, the aim of this study was to investigate the geochemistry of ultramafic soils in terms of their possible impacts on the composition of surrounding waters. Previously, the mineralogical source and the association of Cr, Ni, and Co with various fractions of

ultramafic soils of Sabah were studied to better understand the potential mobility of these elements and their release into the surface water (Tashakor 2014; Tashakor et al. 2017). The current study provides further insights and a broader perspective in Southeast Asia by including new results from Peninsular Malaysia, and by combining geochemical indices and statistical methods to assess the elemental content relationship between ultramafic soils and surface waters.

Material and methods

Study areas

This study focused on ultramafic terrains in Peninsular Malaysia and in Sabah on the Island of Borneo (Figs. 1 and 2). The studied outcrops in Peninsular Malaysia are located at Cheroh (N 03° 53′, E 101° 48′) and Batu Malim (N 03° 58′, E 101° 46′) in Pahang State, Bukit Rokan (N 02° 4′, E 102° 22′) and Petasih (N 02° 59′, E 102° 11′) in Negeri Sembilan State. The outcrops in Sabah are located near Ranau (between N 5° 57′ 6° 02′ and E 116° 40′ 116° 45′). Ultramafic formations of Peninsular Malaysia comprise of several isolated outcrops in a NNW-SSE direction parallel to Bentong- Raub Central Malaya suture zone which is over approximately 20 km wide (Hutchison et al. 2009). This zone represents the closure of the Devonian to Middle Triassic Paleo-Tethys Ocean, resulted by subduction of Gondwana-derived Sibumasu beneath Indochina terrane (Hutchison et al. 2009). The outcropped ultramafic massifs are small and discontinuous appearing as hilly landscapes (Gobbett et al. 1973). The Bukit Rokan region is the most accessible site, where the ultramafic body occurs within the chert-argillite in fault contact with the Kepis Formation (Yeap 1986). The ultramafics of this area are commonly sheared, are strongly weathered, and led to the formation of Geric Ferralsols (Blaterites). At the Petasih site, the ultramafics are highly foliated, sheared, and faulted, and only a small part of this massif was accessible and sampling was performed on the road cut outcrop. The Cheroh site is the largest ultramafic outcrop in Peninsular Malaysia (Richardson 1939) and extends for about 20 km long and is 6 km wide near Raub. The ultramafics are sheared and foliated and accompanied by schist, phyllite, and meta-conglomerate. Similar to other sites, the ultramafics of Cheroh are strongly weathered and produced Geric Ferralsols. At the Batu Malim site, distinctive Geric Ferralsols occur; and locally, the serpentinite is exposed in an active quarry face.

The ultramafics in Sabah are widespread covering an area of ~ 3500 km^2 (Repin 1998). The key study area is located near Ranau, approximately 128 km from the state capital Kota Kinabalu. At Ranau, serpentinized ultramafic formations cover about 41 km^2 (Hing 1969), and the main rock types in the area are tremolite peridotites and spinel lherzolites (Hutchison 2005) with varying degrees of serpentinization (Tashakor et al. 2017; van der Ent et al. 2018). The peridotites have been subjected to intense serpentinization and weathering, and are often difficult to recognize in the field. Serpentinized peridotites are intruded by diabasic dikes and associated with greenschists and amphiblites, which are characteristic rocks of subduction zones.

Sampling of soil and water

In total, 27 soil samples were collected that comprised of four samples from each of the sites at Bukit Rokan (BR), Petasih (PS), and Batu Malim (BM), three samples from Cheroh (CH), and 12 samples from Ranau, surrounding the villages of Kinaratuan, Lohan Skim 1 and 2, Lohan Ulu, and Tuhan. The soil samples were collected from the upper horizon (< 20 cm depth) and organic litter was removed. Soil samples were air-dried, crushed, and passed through a 2-mm plastic sieve. Seven surface water samples (two samples from each region of BR, PS, and BM and one sample from CH) were collected from rivers flowing over ultramafics of Peninsular. In Sabah, the rivers Bongkud, Liwagu, Lohan, Napatau, and Takorek were sampled (total of eight samples). Although, the current study focuses on surface water composition; three seepage waters were also

collected by hand pumping through a plastic pipe, for comparison purposes. The pH and electrical conductivity (EC) were measured in the field using a handheld instrument

(Lovibond SensoDirect 150). Water samples (150 mL) were kept in pre-washed polyethylene containers, and 2 mL of 70% high-purity HNO_3 was added to each bottle to preserve the samples and avoid precipitation of oxyanions.

Soil physical and chemical characterization

The particle size distribution (PSD) of soil samples was determined using the hydrometry method (BS 1377: 2:9.4 1990a). The pH was measured in a 1:2.5 (w:v) soil: water suspension (BS 1377: Part 3:9.0 1990b). The cation exchange capacity (CEC) was determined by summation of Ca, Mg, K, Na, and titratable acidity, all extracted with 1 M ammonium acetate (CH3COONH4) (ASTM D4319 1984). The solutions were filtered through membrane filters (45 μm) and analyzed by ICP-MS (Perkin-Elmer ELAN 9000).

Geochemical and mineralogical analyses

Soil samples were powdered to < 30 μm and processed to fused beads with 0.5 g of sample plus 5 g of sodium metaborate flux (Johnson-Matthey Spectroflux 110). In addition, pressed powder pellets composed of 1 g of sample with 6 g of pure boric acid powder were also prepared (Tashakor 2014). The fused beads and powder pellets were analyzed with X-ray fluorescence spectroscopy to determine the total chemical composition using a Bruker S8 Tiger instrument with a Rh-source. Water samples were filtered through membrane filters (45 μm) and 24 elements (As, Ba, Be, Ce, Cd, Co, Cr, Cu, Fe, Ga, In, K, Li, Mg, Mn, Na, Ni, Pb, Rb, Se, Sr, U, V, Zn) were analyzed by ICP-MS (Perkin-Elmer ELAN 9000). X-ray diffraction (XRD) analysis of air-dried, pulverized, and sieved soils (< 2 mm) was performed on a D8 advance Bruker AXS diffractometer. The analyzing radiation was Cu K-alpha with wavelength of 1.5406 Å (0.15406 NM). X-ray diffractograms were collected on powder samples within the 2θ range [5°–60°], with
0.02/0.1 s step.

Geochemical indices

Geoaccumulation index (Igeo)

The geoaccumulation index (Igeo) (Muller 1969) has been successfully applied to evaluate contamination and is expressed as:

Igeo ¼ Log2 ðCn=1:5 BnÞ ð1Þ

Where Cn is the concentration of the measured element in the sample and Bn is geochemical background value. Seven classes of Igeo describe the levels of soil contamination (Table 1).

Enrichment factor (EF)

The enrichment factor of each element in soil is defined as the ratio of relative concentration of the target (Ci) element and the reference element (CSc) in the soil sample to the relative background concentrations of the target element (Ci) and reference element (CSc) (Echevarria et al. 2006):

EF ¼ ½Ci=CSc]sample=½Ci=CSc]background ð2Þ

Due to the least variation, titanium (Ti) was selected as the reference element in this study. Five levels of enrichment (Qingjie et al. 2008) are shown in Table 1.

Concentration factor (CF)
The Concentration factor is the quotient of concentra- tion of each element in the soil sample (Cn) and the concentration of the same element in the reference soil (Bn) (Dung et al. 2013):

CF ¼ Cn=Bn ð3Þ

Commonly, shale, upper continental crust, or local background values are used as reference material; however, in this study, the World Average Shale Value (ASV) (Turekian and Wedepohl 1961) was used to calculate the EF and CF. The pollution status of elements is classified into four levels from unpolluted to very polluted (Table 1).

Data quality assurance
The precision of the measurements was verified by duplicate analysis of each sample, whereas the accuracy of the X-ray fluorescence spectroscopy was assessed by analyzing certified reference materials with varying SiO2 contents (USGS-BCR-2, SO-2, W-2a, CANMET SY-2, and CRPGGSN) (Tashakor and Hamzah 2011). The precision of the ICP-MS analysis was assessed by analyzing an international reference standard (STD 125 μg L^{-1}) five times, which gave a standard deviation of less than 1.6%. The detection limits for most elements were 0.05 and 0.1 μg L^{-1} for soil and water samples, respectively. The reliability of the X-ray diffractometry was checked by analyzing the International Standard for corundum mineral.

Statistical methods
The raw analytical results were compiled for descriptive and multivariate statistics using Microsoft Excel and IBM©SPSS 23.0 software. The distribution of data for the assumption of normality was tested with the Shapiro-Wilk's test ($p < 0.05$). Due to the non-normal distribution of the data, non-parametric statistics were used. Multivariate statistical methods of correlation and factor analysis are widely used in environmental studies (Tahri et al. 2005; Franco-Uría et al. 2009; Lu et al. 2010). In the current study, the degree of correlation among the measured elements was computed with Spearman's correlation matrix and correlation coefficients. In factor analysis, different groups of elements were classified based on the concept of communality for each element. The varimax rotation method and rotated factor loadings, communalities, and the proportion of the variance were calculated.

Results and discussion

Physico-chemical characteristics of soils
The soils were slightly acidic, with a mean value of pH 5.8 (Table 2). The pH ranged 5.2–7.2 in accordance with soils derived from mafic and ultramafic rocks (pH 5.1–6.3) in tropical regions (Brearley 2005; Massoura et al. 2006; Garnier et al. 2009; van der Ent et al. 2018) where alkaline and calc-alkaline elements are leached. However, soils with values over pH 9 have also been reported in Sabah on fragmented eroded serpentinite (van der Ent et al. 2018). The highest pH value in this was found in sample S6, and all other values were <pH 7. No significant difference was found in pH values in the sampling areas (Table 2). Silt was the main fraction in all the soil samples, except for PS1 from Petasih and BM3 from Batu Malim, which were mainly composed of clay (55%) and sand (67%), respectively (Table 2). The soil textures were thus classified as silty

loam to silty clay loam and clay (Soil Survey Division Staff 1993). The main mineral constituent of the soil samples was quartz, which was found in most samples and explains the silty texture of soils (Tashakor 2014). The soils had varying cation exchange capacities (CEC) with a mean of 9.33 $cmol^{(+)}\ kg^{-1}$, which is lower than reported from ultramafic soils of the Czech Republic (25.3 cmol(+) kg^{-1}), France (12.9–16.6 $cmol^{(+)}\ kg^{-1}$), and Albania (25.4 $cmol^{(+)}kg^{-1}$), but higher than the CEC reported from New Caledonian ultramafic soils (1.4 $cmol^{(+)}\ kg^{-1}$) (Massoura et al. 2006). The CEC of the samples in this study were similar to those of the soils at Mesilau (partially serpentinized tremolite-rich peridotite) and at Bambangan (serpentinite) reported in van der Ent et al. (2018), which are typical CEC values for acidic, silty loamy soils (Holmgren et al. 1993). The CEC was dominated by exchangeable Mg^{2+} with a mean of 8.65 $cmol^{(+)}\ kg^{-1}$ contributing to > 90% of the total CEC; therefore, the B(hyper)magnesic qualifier in WRB soil classification (IUSS Working Group WRB 2015) applies when the exchangeable Mg exceeds exchangeable Ca. Sample PS1 (CEC = 23.7 $cmol^{(+)}\ kg^{-1}$) and sample PS4 (CEC = 23.0 $cmol^{(+)}\ kg^{-1}$) had the highest CECs. A higher CEC implies a higher capacity for immobilizing metal ions (Dube et al. 2001). The lowest CEC was found in sample BM3 (CEC = 1.2 cmol(+) kg^{-1}). The content of clay size fraction in soils showed a significant correlation (r = 0.73) with the CEC values. The identified clay minerals were of the kaolin type, mainly kaolinite and to some extent nacrite (as accessory phases) (Tashakor et al. 2015). The kaolinite could be responsible for the variation in the CEC value, but the studied soils contained only very small amounts of kaolinite which cannot effectively change the result of the CEC. The low amount of CEC in the studied soils may also be attributed to the dominance of Fe-oxy-hydroxide minerals. This is also the case in New Caledonia (Becquer et al. 2001) and other tropical regions with intensive weathering of soils (Echevarria 2018).

Mineralogical composition of soils

The mineral assemblage of ultramafic soils from Sabah and Peninsular Malaysia (Tashakor et al. 2015; Tashakor 2017) showed typical features of tropical soils with oxide and hydrous oxides of Mg and Fe, in particular hematite and goethite. Aluminum hydroxide was common in the soils from Sabah. The ultramafic soils contained different types of spinels, chromite, and cochromite. Clinochlore and maghemite were abundant and gibbsite was common in the Sabah soils, whereas these minerals were absent in the Peninsular Malaysia soils. Inherited serpentine minerals (lizardite and antigorite) were also recognized. Quartz was found in almost all of the soil samples from Peninsular Malaysia. The association of quartz with serpentine minerals occurs as a result of the release of SiO_2 during the near- surface serpentinization process. Quartz + serpentine is a stable assemblage at low temperatures, where conversion of olivine to serpentine or serpentine to clay minerals or talc happens (Streit et al. 2012; Evans 2008; Pirajno 2009). Non-magnesian clay minerals (i.e., kaolinite) were found in minor amounts in some of the soil samples. Leaching of alkali and alkali earth elements has prevented the formation of smectite and nacrite minerals.

Geochemical composition of ultramafic soils

The mean SiO_2 content in the ultramafic soils was 25.1 wt% (Table 2). Overall, the soil samples from Sabah had lower SiO_2 contents compared with those from Peninsular Malaysia. Tashakor (2014) reported that the main silica-bearing minerals in Malaysian ultra- mafic soils are quartz and kaolinite, with minor amounts of lizardite, montmorillonite, and nacrite. Sample BR1 had the lowest SiO_2 content and did not have silica-bearing minerals (XRD results, Tashakor 2014), while PS4 with 30.7 wt% and BR3 with 32.9 wt% SiO_2 had quartz and kaolinite as the main silicate mineral. Therefore, the SiO_2 content does not correspond to the presence of free quartz in the samples. The mean Al_2O_3 and Fe_2O_3 were 13.3 and 31.2 wt%, respectively, in an opposite trend with the concentration of MgO (mean 11.7 wt%) (Table 2). Overall, 66% of the samples contained high Al_2O_3 (11.3–26.9 wt%) and Fe_2O_3 (23.8–55.7 wt%), while these samples were low in MgO (0.21–0.60 wt%). The other 33% of samples had virtually no Al_2O_3 (0.20–0.51 wt%) or Fe_2O_3 (0.02– 0.10

wt%) and were high in MgO (49.2–65.9 wt%). This may be related to the weathering and pedogenesis of ultramafics through which clay minerals destabilize, and thus, highly mobile elements (Si and Mg) were leached from the soil profile at the early stages of soil formation (Echevarria 2018). Soils in well-drained profiles consequently become enriched in Al and Fe, as is typical in tropical climates (Brooks 1987; Caillaud et al. 2009; Echevarria 2018; van der Ent et al. 2018). According to the XRD analysis (Tashakor 2014), Fe mainly occurred in the form of goethite and hematite. These minerals were the most frequent form of Fe-oxides and responsible for the red color—Brhodic qualifier (IUSS Working Group WRB 2015)—of the surveyed soil profiles. The main Al- bearing mineral in the studied soils was kaolinite, associated with some minor phases of montmorillonite and corundum. No significant differences were observed between the two regions regarding their Al_2O_3 and Fe_2O_3 contents. The mean concentration of CaO was very low (0.15 wt%) as were the Na_2O (0.13 wt%), K_2O (0.25 wt%), and P_2O_5 (0.12 wt%) concentrations (Table 2). Again, this is related to the leaching out of these elements through weathering and soil formation. However, CaO, Na_2O, and P_2O_5 were considerably higher in the Peninsular Malaysia soils, while K_2O was higher in the ultramafic soils from Sabah.

Most of the 20 trace elements analyzed occurred at low concentrations. This applies to As, Ba, Ga, Hf, La, Nb, Pb, Rb, Sr, Th, U, Y, Zn, and Zr, which have no environmental implications in this study, and were omitted in further analyses. The studied soils contained relatively high amounts of Cu and Zn with mean values of 43 and 87 mg kg^{-1}, respectively (Table 2). These concentrations exceeded the Upper Continental Crust values given by McLennan (2001), and is indicative of mineralization in this region. Mineral resources of Cu are prevalent in mafic-ultramafic massifs throughout the world (Coleman 1977), including in Turkey (Akinci 2014), Cyprus, Oman (Mahfoud and Beck 1997), Iraq (Yassin et al. 2015), USA (Peterson 1984), and Brazil (Raous et al. 2013). Therefore, the relatively high con- centration of Cu in this study is attributed to disseminated mineralization of Cu in these units. The most striking, among the trace elements, are the high concentrations of Cr, Ni, and Co in the soils (Table 2). The total content of Cr and Ni ranged between 1248 and 27,900 mg kg^{-1} and 189 and 4800 mg kg^{-1}, respectively, and the measured range of Co was from 35 to 464 mg kg^{-1}. These contents were notably higher compared to the Upper Continental Crust (Co 17 mg kg^{-1}, Cr 83 mg kg^{-1}, and Ni 44 mg kg^{-1}) (McLennan 2001). Chromium had a mean value of 11,400 mg kg^{-1}, while the world average soil Cr content is 200 mg kg^{-1} (Bourrelier et al. 1998). The global background of Ni in soils is < 100 mg kg^{-1} (Kabata-Pendias 2001), although values of more than 10,000 mg kg^{-1} have been reported from some ultramafic soils (Brooks 1987; Hseu 2006). In this study, the mean Ni concentration was 1120 mg kg^{-1}. The mean Co concentration was 166 mg kg^{-1}, which is higher than that of the surface soil Co 4.5–12 mg kg^{-1} (Kabata-Pendias and Mukherjee 2007). Chromium, Ni, and Co concentrations in ultramafic soils of the study area (Table 2) were comparable with other reports on the ultramafics in Sabah (van der Ent et al. 2018), India (Rashmi et al. 2009), Oman (Godard et al. 2000), Greece (Skordas and Kelepertsis 2005), and Iran (Ghaderian and Baker 2007). However, the ultramafic soils of this study had lower values than reported from New Caledonia with 31,000 mg kg^{-1} Cr and the local geology did have a significant effect on the concentrations of Ce, Co, Cr, Cu, Nb, Ni, and V in the soils (p values < 0.05). These elements prevail in soils from Sabah, except for Co and V which are relatively more dominant in the Peninsular Malaysia soils. The higher content of Co can be attributed to the presence of cochromite mineral, as the main cobalt-bearing mineral, in all of the Peninsular Malaysia soil samples (Tashakor et al. 2015). The elemental differences between the Sabah and Peninsular Malaysian soils may be explained by differences in the tectonic setting of the parent ophiolitic sequence, petrogenetic processes, and petrology of the exposed ophiolitic section. Finally, As, Ba, Ga, and Zn were not statistically different between Sabah and Peninsular Malaysia (Table 3). A detailed comparison between the concentrations of the elements Cr, Ni, and Co in the four studied areas in Peninsular Malaysia and Sabah is provided by Tashakor (2014).

Geochemical composition of waters

The statistical analysis of the chemical analyses of Pen- insular Malaysia (n = 7) and Sabah (n = 8) surface and subsurface waters (n = 3) is detailed in Table 4. Twenty- four elements were measured in water samples. The concentrations of Be, Cd, Ga, In, Pb, Rb, Se, and U were below the detection limit in almost all of the samples (Pb was around DL, 3–8 μg L^{-1} for three samples from Peninsular Malaysia). These elements are predominant in areas with granite rocks and not expected to be higher compared to ultramafic outcrops. The very high concentration of Mg (Table 4) in water samples is conceivably related to the ultramafic rocks and soils in both Peninsular Malaysia and Sabah. Calcium was not related to ultramafics, but to metamorphic rocks, contributing as major sources of this element in the water samples. Iron was slightly higher in the Sabah water samples corresponding to a similar proportion in the rock units of both regions. However, the higher value can also be attributed to the widespread occurrence of Fe-oxide minerals (goethite and hematite) in the soil profiles. Significant concentrations of Mn in the Peninsular Malaysia waters (Table 4) are in accordance with the local soil geochemistry. The content of Cu in the waters of Sabah is considerably higher than that in the Peninsular Malaysia waters. This reflects the geochemistry of the underlying soils, where Cu is 40 times more enriched in the soils from Sabah compared to those from Peninsular Malaysia. Copper and Zn in Peninsular Malaysia rivers ranged between 2.0 and 13 μg L^{-1} and 4.0 and 5.0 μg L^{-1}, respectively, while in Sabah rivers these elements ranged from 42 to 326 μg L^{-1} for Cu and 20 to 80 μg L^{-1} for Zn. This emphasizes the role of the local geology on trace element geochemistry of waters. The high concentrations may be related to the occurrence of Cu and Zn mineralization in the pathway of the streams. The highest Cu concentrations (1650 μg L^{-1}) and Zn (134 μg L^{-1}) were found in a subsurface water sample (W4) taken from near Ranau in Sabah (Table 4). There is likely to be an influence from the Mamut copper mine and Cu-rich acid mine drainage that drains from the site close to the area (van der Ent and Edraki 2018).

The concentration of Cr in the rivers flowing over ultramafic outcrops of Peninsular Malaysia and Sabah were in the range of 2.0 to 21 μg L^{-1} and 4.0 to 14 μg L^{-1}, respectively, with a mean value of about 8.5 μg L^{-1}. This is comparable to reported values from Greek ophiolites (Voutsis et al. 2015). However, the subsurface waters in the Malaysian ultramafics contained significantly higher Cr, ranging from 23 to 172 μg L^{-1} with a mean of 91 μg L^{-1} (Fig. 3). Nickel varied little in Peninsular Malaysia (4.0– 48 μg L^{-1}) and Sabah (11–94 μg L^{-1}) rivers, with somewhat higher concentrations in the latter. The con- tent of Ni is much higher in subsurface water, with up to 936 μg L^{-1} (Fig. 3). This is substantially higher than the maximum Ni values in subsurface waters reported else- where in Greece (18 μg L–1, Voutsis et al. 2015) and Pakistan (141 μg L^{-1}, Shah et al. 2012). Cobalt is low in most of the samples, indicating the low concentration of this element in the lithological units. The highest concentrations of Co in the rivers of Peninsular Malaysia and Sabah were 3.0 and 7 μg L^{-1}, respectively, but much higher concentrations were found in subsurface waters (mean of 11.3 μg L^{-1}, maximum of 22 μg L^{-1}) (see Table 4 and Fig. 3). Limited information is available in the literature on the effect of ultramafic soils on surface water composition. Vardaki and Kelepertsis (1999) reported ranges of 19–476 μg L^{-1} for Cr, 19–24 μg L^{-1} for Ni, and <5 μg L^{-1} for Co in river water passing over the ultramafic massif of Triad in Greece. The average con- centration of Cr in river water worldwide is 0.7 μg L^{-1}, with a range of 0.04–1.3 μg L^{-1} (Kabata-Pendias and Mukherjee 2007). In drinking water, however, Cr con- tent changes from 0.4 to 8.0 μg L^{-1}, with an average of 1.8 μg L^{-1} (ATSDR 2002). The concentration of Ni in river water ranges between 0.15 and 10.4 μg L^{-1}, while the world average value is 0.8 μg L^{-1} (Gaillardet et al. 2003). The world average value of Co in river water is 0.15 μg L^{-1} (Kabata-Pendias and Mukherjee 2007). The maximum Cr value (21 μg L^{-1}), Ni (94 μg L^{-1}) and Co (7.0 μg L^{-1}) in stream samples were lower than the maximum permissible values (Cr 50 μg L^{-1}, Ni 100 μg L^{-1}, Co 50 μg L^{-1}) proposed by the Interim National Water Quality Standards of Malaysia (INWQS 2006), as shown in Table 4. The elemental composition of water samples was also compared with the World Health Organization (WHO 2006) standard of 50 μg L^{-1} Cr and

70 μg L^{-1} Ni (Table 4). The Cr, Ni, and Co in all of the streams flowing over ultramafic soils fell within these permitted^ INWQS thresholds and the majority were within the WHO standards. The high Cu concentrations in Sabah river water is still below the WHO standard of <2000 μg L^{-1}. Other elements in surface water samples were also within these permissible limits. Therefore, based on the published standards, these streams overrunning ultramafic outcrops, limited by the sampling constraints, appear safe for both drinking water and irrigation. Nevertheless it is conceivable that more comprehensive investigations will reveal values in excess of threshold standards. The subsurface waters in ultramafics are enriched in Cr and Ni, and exceed the standards (Table 4). So, the question arises how to deal with naturally contaminated waters in ultramafic watersheds. At the moment, few ecotoxicological studies have been carried out on ultramafic aquatic environments.

Geoaccumulation and concentration factors

The geoaccumulation index for trace elements in ultra- mafic soils was calculated (Table 5) and shown in boxplots (Fig. 4). The majority of the analyzed soil samples (85%) fell in class 6 of the 6-point scale Igeo for Cr, with the minimum and the maximum observed Igeo values of 3.2 and 7.7, respectively, which indicates an extreme level of contamination for all of the ultramafic soils. The soils were also moderately to strongly contaminated (Igeo classes 4 and 5) with Ni and Co, with the Igeo ranging from 0.9 to 5.5 and 0.3 to 4.0, respectively. Comparatively, the soil samples of Sabah have higher Igeo values for Cu, Cr, and Ni, and lower values for Co and V. Considering the enrichment factor, Cr is the most enriched element in soils with a EF mean value of 638. Most the analyzed soils (92%) have high enrichment in Cr. The EF for Ni had a wide range from 1 to 243, where 37, 33, and 22% of samples fell within significant enrichment (6.1 < EF < 18.3), very high enrichment (21.2 < EF < 37.7), and extremely high enrichment (101 < EF < 951) categories, respectively. Fourteen of the 27 analyzed soil samples fell in the category of significant enrichment^ for Co, with EF values ranging from 5.2 to 19.7. The rest of the samples had various levels of enrichment: moderate enrichment (2.3 < EF < 4.7), very high enrichment (20.9 < EF < 28.1), and extremely high enrichment (46.6 < EF < 936), respectively, in 15, 19, and 15% of the soil samples. A similar result was observed for V with the mean EF value of 10.1. The mean EFs of the elements decreased: Cr > Ni > Co > V (Table 5). Similar to the results of enrichment factor analysis, Cr and Ni showed the highest contamination with an average contamination factor (CF) of 126.8 and 16.4, respectively (Table 5). The CF value for about 70% of the samples ranged from 6.0 to 24.4, which indicates high level of contamination. Six of the soil samples were within the category of considerable contamination for Co (4.89 < CF < 5.89). Soils were considerably contaminated by V with the respective mean CF value of 4.8.

Bivariate statistics

Since the correlation coefficient is a function of the linear interrelationship of the variables, normal distribution of elements was investigated by Shapiro-Wilk test, prior to the correlation test. The Spearman's correlation matrix was computed for 21 pairs of major oxides and trace elements (Table 6). The SiO_2 content has a moderate positive correlation with CaO, MnO, and K_2O ($p < 0.01$). The correlations between SiO_2 and Zr and Zn were strongly positive, indicative of their enrichment and geochemical association in more felsic lithologies. In general, these elements occur in lower concentrations in mafic-ultramafic rocks (Frost and Frost 2013). Fe_2O_3 and MnO did not have a significant correlation with any other element, due to their different origins, host minerals, and their modes of transportation and retention in soil components. TiO2 was strongly related to Al_2O_3 and Ga. These are associated elements in most geochemical environments particularly because of their behavior dur- ing surface weathering (Guilbert and Park 2007). There were strong positive linear correlations between the element pairs MgO-Zn, CaO-K_2O, CaO-Zr, K_2O-Zr, Co-P_2O_5, and Ni-Zn. These pairs of elements mostly produce soluble ions and move freely in solution in surface and ground waters.

Chromium and Ni form other highly correlated pairs, however Co has a different behavior and has a moderate association with MnO. The previous study by Tashakor (2017) showed that serpentine minerals, chromite, and other spinel minerals are the main sources for Cr and Ni, while Co is chiefly bound in the Mn-oxide fraction of the ultramafic soils. Hence, in spite of being geochemically ultramafic-mafic elements (Guilbert and Park 2007), Cr and Ni do not display statistically significant positive correlations with Co. Many of the correlation coefficients are moderate including Al_2O_3 Cu, MgO-Na_2O, Ni-MgO, and Ce-Cu (Table 6).

Different results emerged for the correlation between elements in the analyzed water samples. Chromium was strongly positively correlated with both Ni and Mg (coefficients of r = 0.74 and r = 0.74). This is related to their shared ultramafic origin. Copper and Zn had significant correlations of r = 0.90, while Ni was strongly associated with Mg (r = 0.70), as established by column leaching experiments on saprolitic and limonitic materials from ultramafic soils in Brazil (Raous et al. 2010), while it showed a moderate correlation with Zn (r 0.477). Water samples were not correlated for many pairs of elements. This may be explained by the fact that the streams run over different types of lithologies, and thus, their chemical composition is inherited from the various types of bed- rocks. It is assumed that compared to runoff waters, seep- age waters, which are considered as groundwater (the vertical lines) are the 1.5 interquartile ranges of the lower and upper quartiles. The elemental concentrations of outlier samples are marked as numbers next to them on the boxplots. Circles are mild outliers and asterisks are extreme outliers percolating in the surface veneer, may provide more reliable data on source regions.

Multivariate statistics

In addition to the correlation coefficient analysis, multi-variate statistics for classifying the geochemical data was used. Four principal components were extracted from the available dataset accounting for about 86% of the total variance considering eigenvalues greater than 1. The results of the factor loading and communalities are shown in Table 7. Factor loadings greater than 0.71 are regarded as excellent, and those smaller than 0.32 are considered poor (Nowak 1998). The KMO (Kaiser-Meyer-Olkin) test showed a reliable value (0.60). Elements for factor analysis were selected among the potentially toxic elements and those which showed significant correlations in the bivariate analysis. In Table 7, the first factor (F1) includes strong associations of MgO, MnO, and Na_2O with high factor loading values of 0.97, 0.95, and 0.79, respectively. Factor 1 (F1) explains 36.4% of the total variance and indicates the geochemical association of soluble (lithophile) elements in soil samples. These elements are normally transferred to soils during the weathering of ultramafic rocks. This group of elements are captured, or incorporated, into the structure of newly formed minerals during pedogenesis. This result is in accordance with the correlations that emerged in the bivariate correlation matrix. Given that Mg is the main cation in ultramafic rocks and soils, a high concentration in the soil samples was expected. Magnesium is found in various minerals of the spinel group, such as periclase, jacobsite, lizardite, clays, and also in numerous solid solution minerals substituting for Fe and associated with Ni, Co, and Al (Cornelis and Dutrow 2007).

Factor 2 (F2) accounts for 25.2% of the total variance, dominated by SiO_2, CaO, and K_2O with significant factor loadings. It covers a group of lithophile elements, which are removed from the soil profile into water systems or infiltrates into the lower profiles of the soil. Therefore, their concentrations are considerably lower in soil in comparison to fresh bedrock. Copper is almost isolated in Factor 3 (F3) accounting for 13.3% of the total variance. Copper indicates disseminated sulphide mineralization, and it is not accompanied by other ore-forming elements, e.g., Zn, Pb, Cd. This can be explained by the fact that ultramafic source rocks are devoid of these base metals (Guilbert and Park 2007). Factor 4 (F4) of the factor analysis, which explains 11.3% of the total variance, is dominated by Cr (0.810) and Ni (0.918). Chromium and Ni are highly enriched and

associated with ultramafic rocks and soils and are hosted by various spinel group minerals. To illustrate the interrelations, the four main factors are plotted in three-dimensional space in Fig. 5, where the associations between elements can be observed.

Conclusion

The ultramafic bedrock of Peninsular Malaysia and Sabah host considerable amounts of Cr, Ni, and Co, leading to enrichment in the soil and surface waters, in comparison with the values in the Upper Continental Crust. Extreme to moderate levels of Cr, Ni, and Co contamination were confirmed by geoaccumulation index, enrichment, and contamination factors. There were significant positively correlated pairs of Cr-Ni and weak association of Co due to the difference in host minerals. The river waters flowing over ultramafic bodies contained significant concentrations of Mg, Mn, and Fe. Following the local geochemistry of the studied regions, Cu and Zn are more enriched in the rivers of Sabah, indicative of the role of regional mineralization. However, rivers interacting with ultramafic bedrocks had minimal influence in terms of the content of Cr, Ni, and Co, and these elements are within the permissible limits for drinking and irrigation waters (WHO). However, a few subsurface water samples were contaminated with Cr and Ni. Factor analysis of the ultramafic soils categorized the lithophile elements of MgO, MnO, and Na_2O in the first factor, indicating their incorporation in weather-produced ultramafic soils, while SiO_2, CaO, and K_2O were grouped together in the second factor, as the elements removed from the soil profile or infiltrate into water system. The assumption of disseminated sulfide mineralization was accentuated by the presence of Cu alone in the third fraction of factor analysis. The association of Cr and Ni in ultramafic soils was displayed in fraction four. It would be interesting to study the pedogenic processes and especially mass transfer in the formation of ultramafic soils in the same areas of this study. Further studies could explore the distribution Cr, Ni, and Co in ultramafic soils at the scale of weathering profiles. In addition, more information on different oxidation states of chromium helps us to understand the level of threat of Cr pollution in the environment. More research on groundwater pollution in relation to the ultramafic soils is needed. Finally, it is recommended to investigate the variation of trace element contents in river and subsurface waters in different seasons and the impact of fluctuations of river discharge and the amount of rainfall on prevailing concentrations.

Acknowledgements

This study was part of the M. Tashakor's Ph.D. thesis, and she wishes to thank Universiti Kebangsaan Malaysia (UKM) and the staff from the School of Science and Technology for support. M. Tashakor also acknowledges Universiti Malaysia Sabah (UMS) for organizing the field- work for sample collection. A. van der Ent is the recipient of a Discovery Early Career Researcher Award (DE160100429) from the Australian Research Council. We thank anonymous reviewers for constructive comments that improved this article.

References

Akinci, O. T. (2014). Ophiolite-hosted copper and gold deposits of southeastern Turkey: formation and relationship with sea-floor hydrothermal processes. Turkish Journal of Earth Sciences, 18(4), 475–509.

Alexander, E. B., & DuShey, J. (2011). Topographic and soil differences from peridotite to serpentinite. Geomorphology, 135(3–4), 271–276.

Alexander, E. B., Coleman, R. G., Keeler-Wolfe, T., & Harrison, S. P. (2006). Serpentine geoecology of western North America: geology, soils, and vegetation. USA: Oxford University Press 528p.

Ashraf, M. A., Sarfraz, M., Naureen, R., & Gharibreza, M. (2015). Environmental impacts of metallic elements: speciation, bio- availability and remediation (434p). Singapore: Springer.

ASTM. (1984). Standard test method for distribution ratios by the short-term batch method. Annual book of ASTM standards (pp. 766–773). West Conshohocken: American Society for Testing and Materials.

ATSDR. (2002). Draft toxicological profile for several trace elements. Atlanta: U.S. Department of Health and Human Services. Agency for Toxic Substances and Disease Registry.

Baioumy, H., Ulfa, Y., Nawawi, M., Padmanabhan, E., & Anuar, M. N. A. (2016). Mineralogy and geochemistry of Palaeozoic black shales from Peninsular Malaysia: implications for their origin and maturation. International Journal of Coal Geology, 165, 90–105.

Becquer, T., Pétard, J., Duwig, C., Bourdon, E., Moreau, R., & Herbillon, A. J. (2001). Mineralogical, chemical and charge properties of Geric Ferralsols from New Caledonia. Geoderma, 103(3–4), 291–306.

Becquer, T., Quantin, C., Rotte-Capet, S., Ghanbaja, J., Mustin, C., & Herbillon, A. J. (2006). Sources of trace metals in Ferralsols in New Caledonia. European Journal of Soil Science, 57(2), 200–213.

Boyd, R. S., Baker, A. J. M., Proctor, J. (2004). Ultramafic rocks: their soils, vegetation and fauna. In: Proceedings of the Fourth International Conference on Serpentine Ecology, Cuba, 21–26 April, 2003. Science Reviews.

Boyd, R. S., Kruckeberg, A. R., & Rajakaruna, N. (2009). Biology of ultramafic rocks and soils: research goals for the future. Northeastern Naturalist, 16(5), 422–440.

Brearley, F. (2005). Nutrient limitation in a Malaysian ultramafic soil. Journal of Tropical Forest Science, 17(4), 596–609.

British Standard Institution. (1990a). Methods of test for soils for civil engineering purposes—BS 1377—part 2:9.4. Particle size analysis. London: British Standard Institution.

British Standard Institution. (1990b). Methods of test for soils for civil engineering purposes—BS 1377—part 3: 9.0. pH anal- ysis. London: British Standard Institution.

Brooks, R.R. (1983). Biological methods of prospecting for minerals. New York: Wiley.

Brooks, R. R. (1987). Serpentine and its vegetation: a multidisciplinary approach (288p). Portland: Dioscorides Press.

Caillaud, J., Proust, D., Philippe, S., Fontaine, C., & Fialin, M. (2009). Trace metals distribution from a serpentinite weathering at the scales of the weathering profile and its related weathering microsystems and clay minerals. Geoderma, 149(3–4), 199–208.

Cheng, C. H., Jien, S. H., Tsai, H., Chang, Y. H., Chen, Y. C., & Hseu, Z. Y. (2009). Geochemical element differentiation in serpentine soils from the ophiolite complexes, eastern Taiwan. Soil Science, 174(5), 283–291.

Coleman, R. G. (1977). Ore deposits in ophiolites. In R. G. Coleman (Ed.), Ophiolites, ancient oceanic lithosphere? (pp. 124–139). Heidelberg: Springer.

Coleman, R. G., Jove, C. (1992). Geological origin of serpentinites. In: Proceedings of the First International Conference on Serpentine Ecology, Davis: Intercept Ltd., University of California.

Cornelis, K., & Dutrow, B. (2007). Manual of mineral science. Hoboken: Wiley Interscience 675p.

Dube, A., Zbytniewski, R., Kowalkowski, T., Cukrowska, E., & Buszewski, B. (2001). Adsorption and migration of heavy metals in soil. Polish Journal of Environmental Studies, 10(1), 1–10.

Dung, T. T. T., Cappuyns, V., Swennen, R., & Phung, N. K. (2013). From geochemical background determination to pol- lution assessment of heavy metals in sediments and soils. Reviews in Environmental Science and Biotechnology, 12(4), 335–353.

Echevarria, G. (2018). Chapter 8: Genesis and behaviour of ultra- mafic soils and consequences for nickel biogeochemistry. In: van der Ent A, Echevarria G, Baker AJM, Morel JL (eds). Agromining: farming for metals, mineral resource reviews. Springer International Publishing. In Press. https://doi. org/10.1007/978-3-319-61899-9_8.

Echevarria, G., Massoura, S., Sterckeman, T., Becquer, T., Schwartz, C., & Morel, J. L. (2006). Assessment and control of the bioavailability of Ni in soils. Environmental Toxicology and Chemistry, 25, 643–651.

Evans, B. W. (2008). Control of the products of serpentinization by the Fe^{2+} Mg^{-1} exchange potential of olivine and orthopyroxene. Journal of Petrology, 49(10), 1873–1887.

Franco-Uría, A., López-Mateo, C., Roca, E., & Fernández- Marcos, M. L. (2009). Source identification of heavy metals in pastureland by multivariate analysis in NW Spain. Journal of Hazardous Materials, 165(1), 1008–1015.

Frost, B. R., & Frost, C. D. (2013). Essentials of igneous and metamorphic petrology. Cambridge: Cambridge University Press 314p.

Ghaderian, S. M., & Baker, A. J. M. (2007). Geobotanical and biogeochemical reconnaissance of the ultramafics of Central Iran. Journal of Geochemical Exploration, 92(1), 34–42.

Gaillardet, J., Viers, J., & Dupré, B. (2003). Trace elements in river waters. Treatise on Geochemistry, 5, 225–272.

Galey, M. L., Van Der Ent, A., Iqbal, M. C. M., & Rajakaruna, N. (2017). Ultramafic geoecology of South and Southeast Asia. Botanical Studies, 58(1), 18.

Garnier, J., Quantin, C., Guimarães, E., Garg, V. K., Martins, E. S., & Becquer, T. (2009). Understanding the genesis of ultramafic soils and catena dynamics in Niquelândia, Brazil. Geoderma, 151(3–4), 204–214.

Georgopoulos, G., Mitsis, I., Argyraki, A., & Stamatakis, M. (2018). Environmental availability of ultramafic rock derived trace elements in the fumarolic-geothermal field of Soussaki area. Greece: Applied Geochemistry In press.

Gobbett, D. J., Hutchison, C. S., & Burton, C. K. (1973). Geology of the Malay peninsula: West Malaysia and Singapore. California: Wiley-Interscience 440p.

Godard, M., Jousselin, D., & Bodinier, J.-L. (2000). Relationships between geochemistry and structure beneath a palaeo-spreading centre: a study of the mantle section in the Oman ophiolite. Earth and Planetary Science Letters, 180(1-2), 133–148.

Guilbert, J. M., & Park, C. F. (2007). The geology of ore deposits. Long Grove: Waveland Press 985p.

Hing, T. T. (1969). Geology and soils of the Ranau-Luhan area, Sabah, East Malaysia. Kuala Lumpur: Department of Geology, University of Malaya 86p.

Holmgren, G. G. S., Meyer, M. W., Chaney, R. L., & Daniels, R. B. (1993). Cadmium, lead, zinc, copper, and nickel in agricultural soils of the United States of America. Journal of Environmental Quality, 22(2), 335–348.

Hseu, Z. Y. (2006). Concentration and distribution of chromium and nickel fractions along a serpentinitic toposequence. Soil Science, 171(4), 341–353.

Hseu, Z. Y., & Iizuka, Y. (2013). Pedogeochemical characteristics of chromite in a paddy soil derived from serpentinites. Geoderma, 202, 126–133.

Hseu, Z. Y., Tsai, H., Hsi, H. C., & Chen, Y. C. (2007). Weathering sequences of clay minerals in soils along a serpentinitic toposequence. Clays and Clay Minerals, 55(4), 389–401.

Hseu, Z. Y., Zehetner, F., Ottner, F., & Iizuka, Y. (2015). Clay- mineral transformations and heavy-metal release in paddy soils formed on serpentinites in eastern Taiwan. Clays and Clay Minerals, 63(2), 119–131.

Hseu, Z. Y., Watanabe, T., Nakao, A., & Funakawa, S. (2016). Partition of geogenic nickel in paddy soils de-rived from serpentinites. Paddy and Water Environment, 14(3), 417–426.

http://amphibiaweb.org/maps/geo-malaysia.html, Accessed: 20 September 2017.

Hutchison, C. S. (2005). Geology of north-west Borneo: Sarawak, Brunei and Sabah. Amsterdam: Elsevier Science 421p.

Hutchison, C. S., Tan, D. N. K., & Malaya, U. (2009). Geology of peninsular Malaysia. Kuala Lumpur: University of Malaya 479p.

INWQS. (2006). Interim national water quality standards of Malaysia (online) http: www.wepa-db. net/policies/law/malaysia/eq_surface.htm (April 2010).

IUSS Working Group WRB. (2015). World reference base for soil resources 2014, update 2015 International soil classification system for naming soils and creating legends for soil maps. World Soil Resources Reports No. 106. FAO, Rome.

Jatmika Setiawan. (2009) Evolusi struktur di jalur Tengah Semenanjung Malaysia, dengan penekanan terhadap Negri Kelantan Ph.D thesis, School of Environmental and Natural Resource Sciences, University Kebangsaan Malaysia. 132p.

Kabata-Pendias, A., & Mukherjee, A. B. (2007). Trace elements from soil to human. New York: Springer 550p.

Kar, D., Sur, P., Mandal, S., Saha, T., & Kole, R. (2008). Assessment of heavy metal pollution in surface water. International journal of Environmental Science and Technology, 5(1), 119–124.

Kierczak, J., Neel, C., Bril, H., & Puziewicz, J. (2007). Effect of mineralogy and pedoclimatic variations on Ni and Cr distribution in serpentine soils under temperate climate. Geoderma, 142, 165–177.

Kierczak, J., Neel, C., Aleksander-Kwaterczak, U., Helios- Rybicka, E., Bril, H., & Puziewicz, J. (2008). Solid speciation and mobility of potentially toxic elements from natural and contaminated soils: a combined approach. Chemosphere, 73(5), 776–784.

Kumar, A., & Maiti, S. K. (2013). Availability of chromium, nickel and other associated heavy metals of ultramafic and serpentine soil/rock and in plants. International Journal of Emerging Technology and Advanced Engineering, 3(2), 256–268.

Lu, X., Wang, L., Li, L. Y., Lei, K., Huang, L., & Kang, D. (2010). Multivariate statistical analysis of heavy metals in street dust of Baoji, NW China. Journal of Hazardous Materials, 173(1), 744–749.

Mahfoud, R. F., & Beck, J. N. (1997). Copper mineralizations in the ophiolite of Oman: the genesis and emplacement relationship with the orogenic movements of serpentinised peridotite. International Geology Review, 39(3), 252–286.

Massoura, S. T., Echevarria, G., Becquer, T., Ghanbaja, J., Leclerc-Cessac, E., & Morel, J. L. (2006). Control of nickel availability by nickel bearing minerals in natural and anthropogenic soils. Geoderma, 136(1–2), 28–37.

Mclennan, S. M. (2001). Relationships between the trace element composition of sedimentary rocks and upper continental crust. Geochemistry, Geophysics, Geosystems, 2(4), 1021.

Muller, G. (1969). Index of geoaccumulation in sediments of the Rhine River. Geological Journal, 2, 108–118.

O'Hanley, D. S. (1996). Serpentinites: records of tectonic and petrological history. New York: Oxford University Press 277p.

Oze, C., Fendorf, S., Bird, D. K., & Coleman, R. G. (2004). Chromium geochemistry in serpentinised ultramafic rocks and serpentine soils from the Franciscan complex of California. American Journal of Science, 304(1), 67–101.

Peterson, J. A. (1984). Metallogenetic maps of the ophiolite belts of the western United States. Reston: US Geological Survey. Pirajno, F. (2009). Hydrothermal processes associated with meteorite impacts. Hydrothermal processes and mineral systems (pp. 1097–1130). Amsterdam: Springer Netherlands.

Qingjie, G., Jun, D., Yunchuan, X., Qingfei, W., & Liqiang, Y. (2008). Calculating pollution indices by heavy metals in ecological geochemistry assessment and a case study in parks of Beijing. Journal of China University of Geosciences, 19(3), 230–241.

Quantin, C., Ettler, V., Garnier, J., & Šebek, O. (2008). Sources and extractibility of chromium and nickel in soil profiles developed on Czech serpentinites. Comptes Rendus Geoscience, 340(12), 872–882.

Rahim, S. A., MdTan, M., & Musta, B. (1996). Heavy metals composition of some soils developed from basic and ultraba- sic rocks in Malaysia Borneo. Science, 2, 33–46.

Raous, S., Becquer, T., Garnier, J., Martins, E. S., Echevarria, G., & Sterckeman, T. (2010). Mobility of metals in nickel mine spoil materials. Applied Geochemistry, 25, 1746–1755.

Raous, S., Echevarria, G., Sterckeman, T., Hanna, K., Thomas, F., Martins, E. S., & Becquer, T. (2013). Potentially toxic metals in ultramafic mining materials: identification of the main bearing and reactive phases. Geoderma, 192, 111–119.

Rashmi BN, Prabhakar BC, Gireesh RV, Nijagunaiah R, Ranganath RM (2009) Nickel anomalies in ultramafic pro- files of Jayachamarajapura schist belt, Western Dharwar Craton. Current Science, 96, 1512–1517

Repin, R. (1998). Preliminary survey of serpentine vegetation areas in Sabah. Sabah Parks Nature Journal, 1, 19–28.

Richardson, J. A. (1939). The geology and mineral resources of the neighbourhood of Raub, Pahang with an account of the geology of the Raub Australian Gold Mine. Kuala Lumpur: Geological Survey of Malaysia 166p.

Schwertmann, U., & Latham, M. (1986). Properties of iron oxides in some New Caledonian oxisols. Geoderma, 39(2), 105– 123.

Shah, M. T., Ara, J., Muhammad, S., Khan, S., & Tariq, S. (2012). Health risk assessment via surface water and sub-surface water consumption in the mafic and ultramafic terrain, Mohmand agency, northern Pakistan. Journal of Geochemical Exploration, 118, 60–67.

Shanker, A. K., Cervantes, C., Loza-Tavera, H., & Avudainayagam, S. (2005). Chromium toxicity in plants. Environment International, 31(5), 739–753.

Skordas, K., & Kelepertsis, A. (2005). Soil contamination by toxic metals in the cultivated region of Agia, Thessaly, Greece. Identification of sources of contamination. Environmental Geology, 48(4), 615–624.

Soil Survey Division Staff. (1993). Soil survey manual. Washington, DC: United States Department of Agriculture.

Streit, E., Kelemen, P., & Eiler, J. (2012). Coexisting serpentine and quartz from carbonate-bearing serpentinized peridotite in the Samail ophiolite, Oman. Contributions to Mineralogy and Petrology, 164(5), 821–837.

Tahri, M., Benyaich, F., Bounakhla, M., Bilal, E., Gruffat, J. J., Moutte, J., & Garcia, D. (2005). Multivariate analysis of heavy metal contents in soils, sediments and water in the region of Meknes (Central Morocco). Environmental Modeling and Assessment, 102(1–3), 405–417.

Tashakor, M. (2014). Geochemistry of serpentinite and its effect on the environment: case study at Peninsular and Sabah Malaysia. Unpublished PhD Thesis. University Kebangsaan Malaysia (UKM). 234 p.

Tashakor, M., Hamzah, M. (2011). An accurate XRF technique for the analysis of geological materials. Proceeding Volume of National Geoscience Conference, hlm. 115. The Puteri Pacific Johor Bahru, Johor, Malaysia. 11–12 June.

Tashakor, M., Yaacob, W. Z. W., Mohamad, H., Ghani, A. A., & Saadati, N. (2014). Assessment of selected sequential extraction and the toxicity characteristic leaching test as indices of metal mobility in serpentinite soils. Chemical Speciation & Bioavailability, 26(3), 139–147(9).

Tashakor, M., Hochwimmer, B., & Imanifard, S. (2015). Control of grain-size distribution of serpentinite soils on mineralogy and heavy metal concentration. Asian Journal of Earth Sciences, 8(2), 45.

Tashakor, M., Hochwimmer, B., & Brearley, F. Q. (2017). Geochemical assessment of metal transfer from rock and soil to water in serpentine areas of Sabah (Malaysia). Environment and Earth Science, 76, 281.

Turekian, K. K., & Wedepohl, K. H. (1961). Distribution of the elements in some major units of the earth's crust. Geological Society of America Bulletin, 72(2), 175–192.

van der Ent, A. (2011). The ecology of ultramafic areas in Sabah: threats and conservation needs. Gardens' Bulletin Singapore, 63, 385–394.

van der Ent, A., Edraki, M. (2018). Environmental geochemistry of the abandoned Mamut Copper Mine (Sabah) Malaysia. Environmental Geochemistry and Health, 40(1):189-207.

van der Ent, A., Baker, A. J. M., Van Balgooy, M. M. J., & Tjoa, A. (2013). Ultramafic nickel laterites in Indonesia (Sulawesi, Halmahera): mining, nickel hyperaccumulators and opportunities for phytomining. Journal of Geochemical Exploration, 128, 72–79.

van der Ent, A., Cardace, D., Tibbett, M., & Echevarria, G. (2018). Ecological implications of pedogenesis and geochemistry of ultramafic soils in Kinabalu Park (Malaysia). Catena, 160, 154–169.

Vardaki, C., & Kelepertsis, A. (1999). Environmental impact of heavy metals (Fe, Ni, Cr, Co) in soils waters and plants of triada in euboea from ultrabasic rocks and nickeliferous mineralisation. Environmental Geochemistry and Health, 21(3), 211–226.

Vithanage, M., Rajapaksha, A. U., Oze, C., Rajakaruna, N., & Dissanayake, C. B. (2014). Metal release from serpentine soils in Sri Lanka. Environmental Monitoring and Assessment, 186(6), 3415–3429.

Voutsis, N., Kelepertzis, E., Tziritis, E., & Kelepertsis, A. (2015). Assessing the hydrogeochemistry of groundwaters in ophiolite areas of Euboea Island, Greece, using multivariate statistical methods. Journal of Geochemical Exploration, 159, 79–92.

Wesolowski, M. F. (2003). Geochemical analysis of the soils and surface water derived from chemical weathering of ultramafic rock, Cornwall, England: trace metal speciation and eco- logical consequences. B.S. thesis, Department of geology, Middlebury College.74p.

WHO. (2006). Guidelines for drinking-water quality. Geneva: Switzerland. Yassin, A., Alabidi, A., Hussain, M., Al-Ansari, N., & Knutsson, S. (2015). Copper ores in Mawat ophiolite complex (part of ZSZ) NE Iraq. Natural Resources, 6(10), 514–526.

Yeap, K. L. (1986). Geology of an area south of Bahau. B.S. thesis, Department of Geology, University of Malaya. 127p. Yuen, H. C. (1996). A study of the distribution and transport of heavy metals in Malaysian rivers and seawater. Kuala Lumpur: Department of Geology. University Malaya 384p.

FIGURES AND TABLES

Fig. 1 Map of Malaysia (http://amphibiaweb.org/maps/geo-malaysia.html). Geological maps of Sabah (Jatmika Setiawan 2009) and the Ranau area (Tashakor 2014) and the sampling locations.

Fig. 2 Locations of the study areas in Peninsular Malaysia: Bukit Rokan, Petasih, Batu Malim, and Cheroh (Peninsular Malaysia geology map is adapted from Baioumy et al. (2016) showing the sample locations (Tashakor 2014)).

Fig. 3 Concentrations of Cr and Ni in surface and subsurface waters in selected samples (CH6, BM11, W4) (in $\mu g\ L^{-1}$).

Fig. 4 Box plots representing the values of geoaccumulation index (Igeo), enrichment factor (EF), and contamination factors (CF) for trace elements in the ultramafic soils from the study areas. The band near the middle of each box represents the median. The bottom and top of the box are the first and third quartiles, respectively. Whiskers (the vertical lines) are the 1.5 interquartile ranges of the lower and upper quartiles. The elemental concentrations of outlier samples are marked as numbers next to them on the boxplots. Circles are mild outliers and asterisks are extreme outliers.

Fig. 5 Factor analysis results in the three-dimensional space of the geochemical data from the study areas.

Table 1 The adjusted grading standard of geoaccumulation index, enrichment factor, and contamination factor of elements in soil

Table 2 Descriptive statistics of physical and chemical characteristics and the concentration of major oxides and trace elements in the ultramafic soils from the study areas.

Table 3 The result of Kruskal-Wallis and Mann-Whitney tests on soil data from the study areas in Peninsular Malaysia and Sabah.

Table 4 Concentrations of trace elements in river and subsurface waters traversing ultramafics in the study areas in Peninsular Malaysia and Sabah.

Table 5 Statistical description of geoaccumulation index (Igeo), enrichment factor (EF), and contamination factors (CF) for the analyzed elements in the ultramafic soils from the study areas.

Table 6 Spearman's correlation matrix of elements in ultramafic soil samples from the study areas in Peninsular Malaysia and Sabah.

Table 7 The rotated component matrix of elements in the ultramafic soils from the study areas.

FIGURE 1

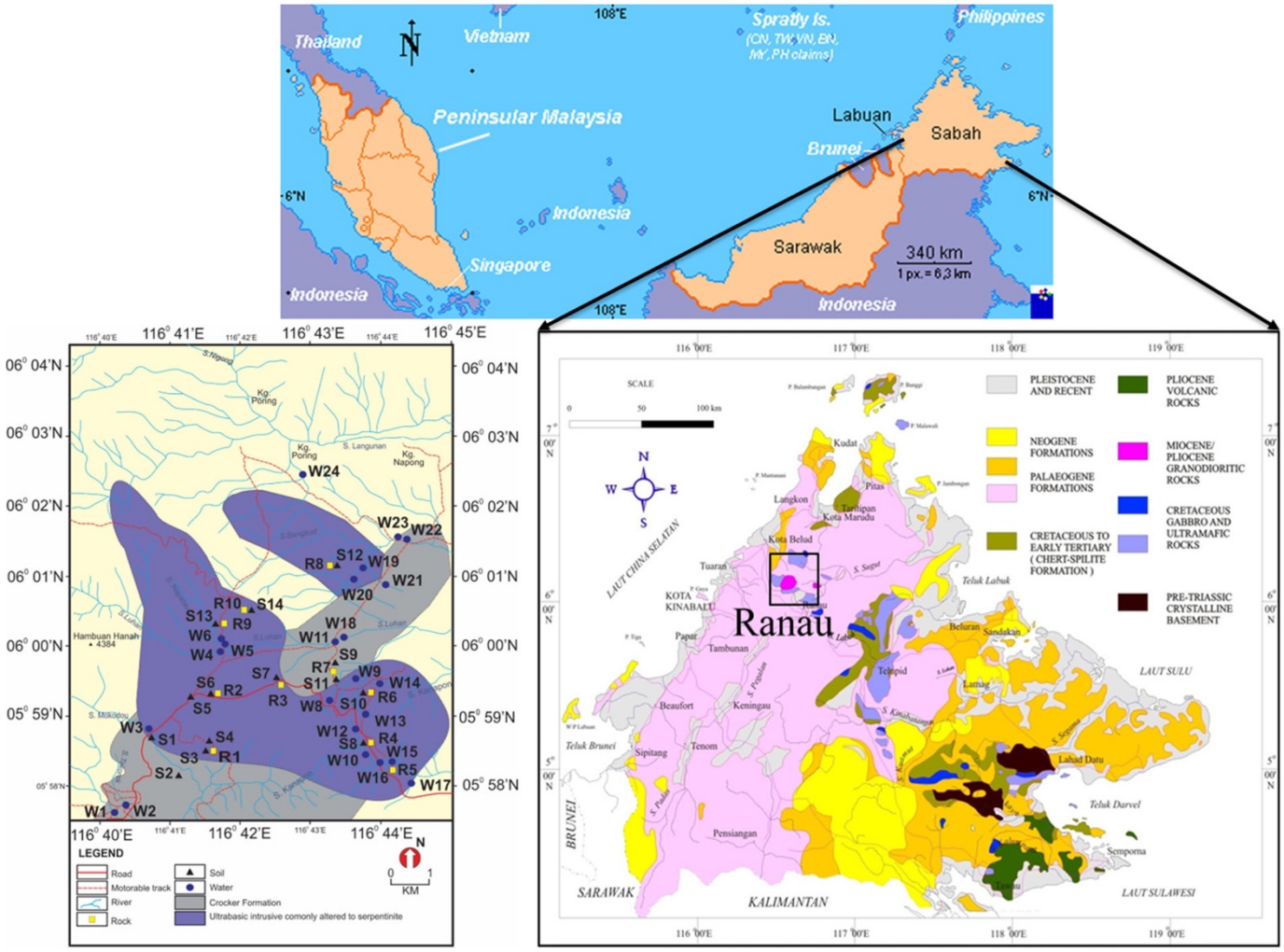
Thailand
Vietnam
108°E
Spratly Is.
(CN, TW, VN, BN, MY, PH claims)
Philippines
Peninsular Malaysia
Labuan
Sabah
Brunei
6°N
Indonesia
Singapore
Sarawak
340 km
1 px. = 6,3 km
Indonesia
108°E
116° 41'E
116° 43'E
116° 45'E
06° 04'N
06° 03'N
06° 02'N
06° 01'N
06° 00'N
05° 59'N
05° 58'N
Kg. Poring
S. Langunan
Kg. Napong
W24
W23
W22
R8
S12
W19
W21
W20
R10
S14
S13
R9
W18
W6
W11
W4
W5
S9
R7
S7
W9
W14
S6
S11
R2
S5
R3
W8
S10
R6
W13
W3
S1
S4
W12
S8
R4
S3
R1
W10
W15
S2
R5
W16
W17
W1
W2
Hambuan Hanah
4384
LEGEND
Road
Motorable track
River
Rock
Soil
Water
Crocker Formation
Ultrabasic intrusive comonly altered to serpentinite
0
1
KM
116° 00'E
117 00'E
118 00'E
119 00'E
SCALE
0
50
100 km
PLEISTOCENE AND RECENT
NEOGENE FORMATIONS
PALAEOGENE FORMATIONS
CRETACEOUS TO EARLY TERTIARY (CHERT-SPILITE FORMATION)
PLIOCENE VOLCANIC ROCKS
MIOCENE/ PLIOCENE GRANODIORITIC ROCKS
CRETACEOUS GABBRO AND ULTRAMAFIC ROCKS
PRE-TRIASSIC CRYSTALLINE BASEMENT
Ranau
Kudat
Pitas
Langkon
Tampian
Kota Maruda
Kota Belud
Tuaran
KOTA KINABALU
Papar
Tambunan
Teluk Labuk
Beluran
Sandakan
Telupid
Lamag
LAUT SULU
Beaufort
Keningau
Teluk Brunei
Sipitang
Tenom
Lahad Datu
Teluk Darvel
Pensiangan
Semporna
Tawau
BRUNEI
SARAWAK
KALIMANTAN
LAUT SULAWESI
LAUT CHINA SELATAN

FIGURE 2

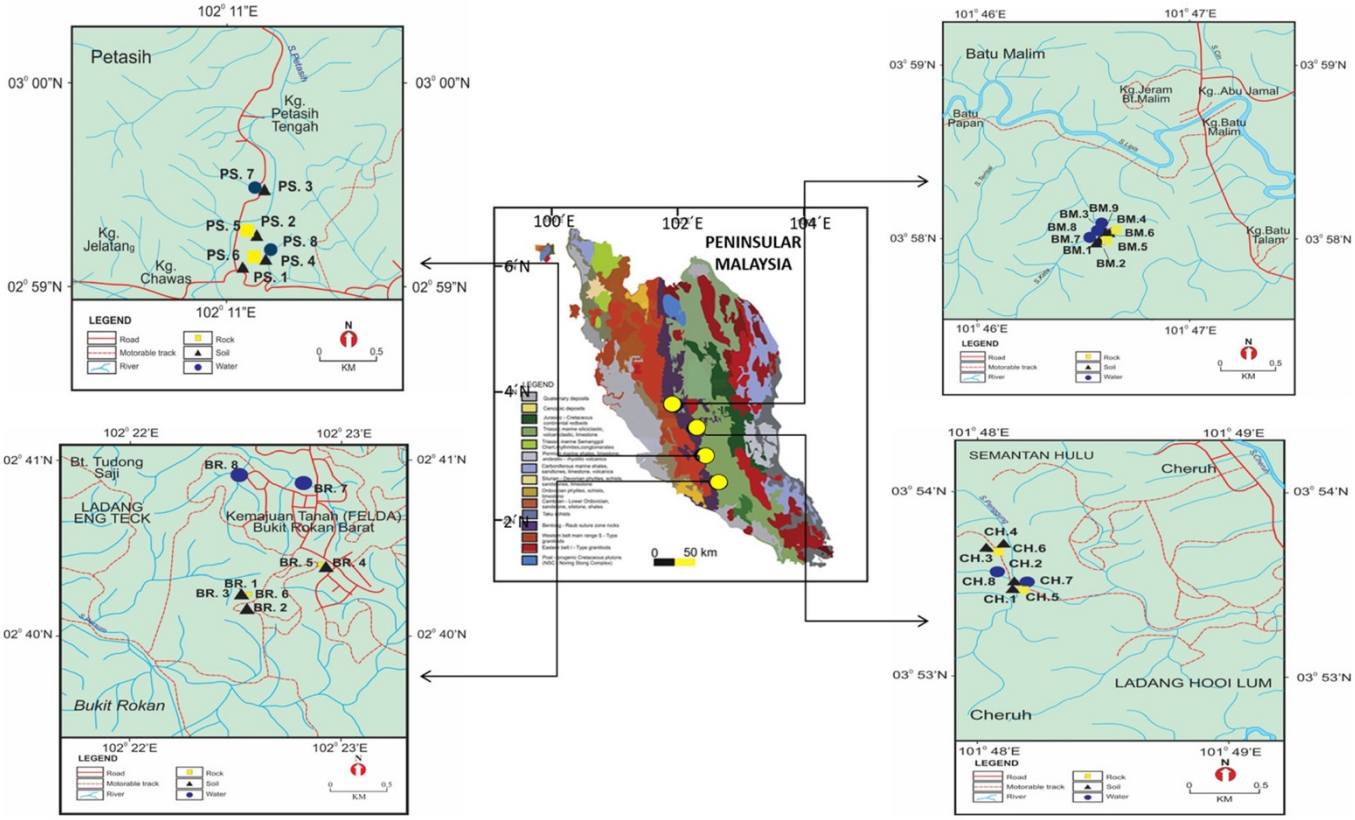

FIGURE 3

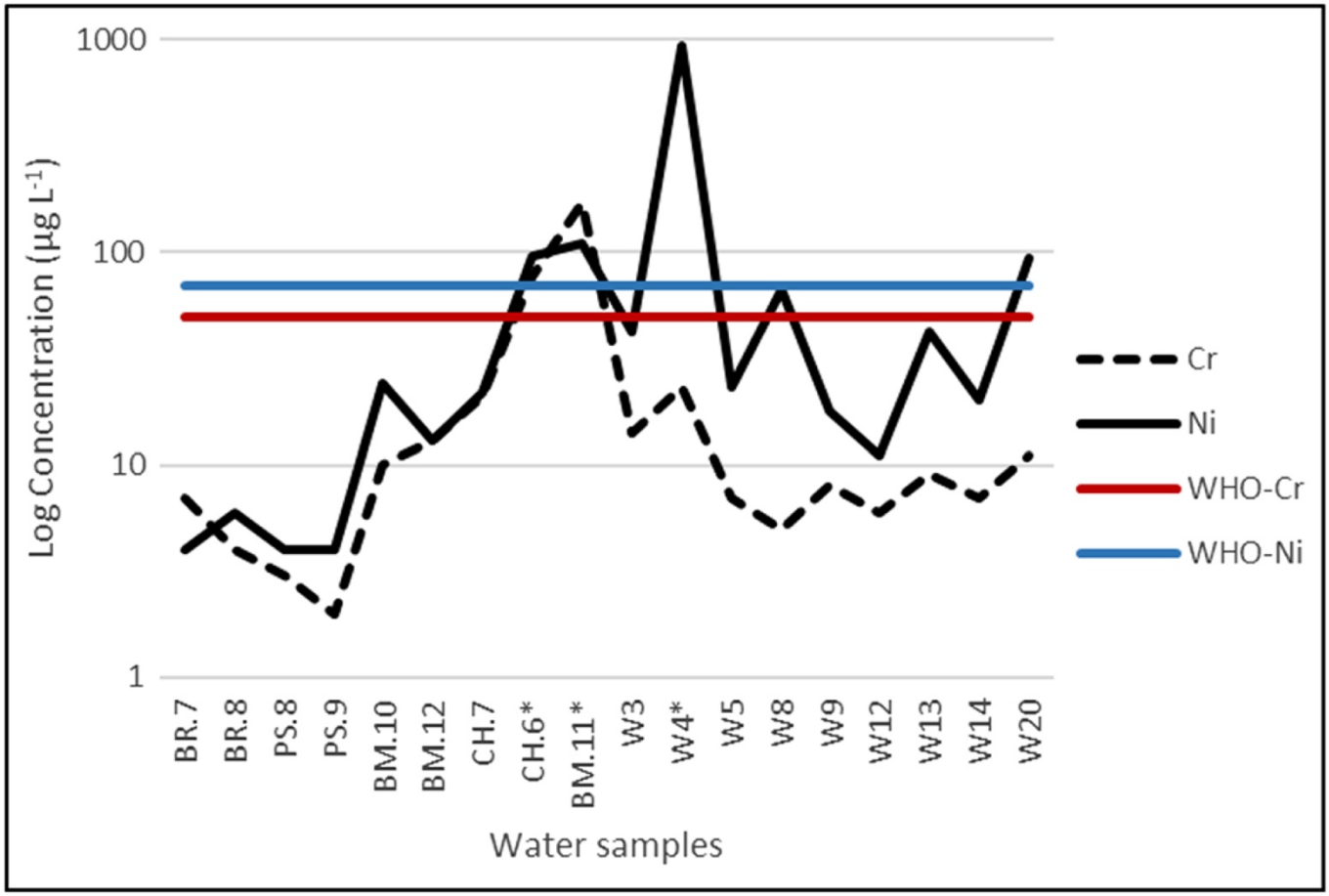

FIGURE 4

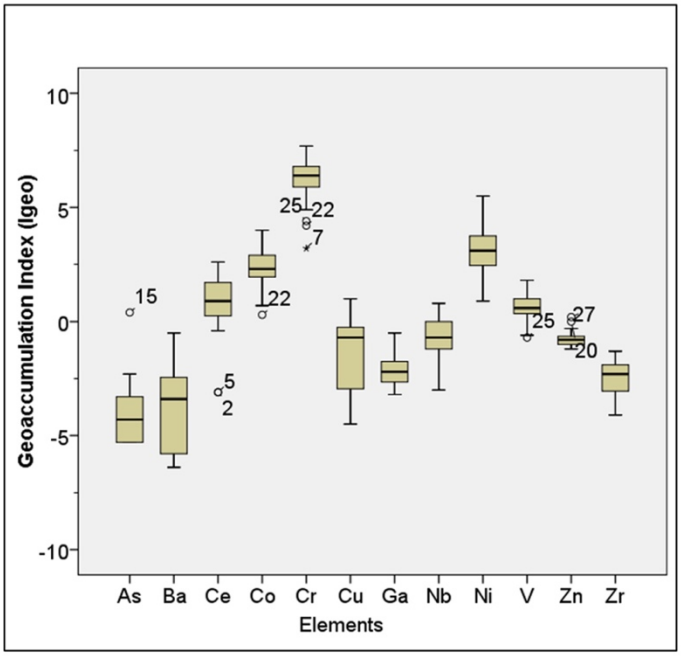
Geoaccumulation Index (Igeo)
10
5
0
-5
-10
As Ba Ce Co Cr Cu Ga Nb Ni V Zn Zr
Elements

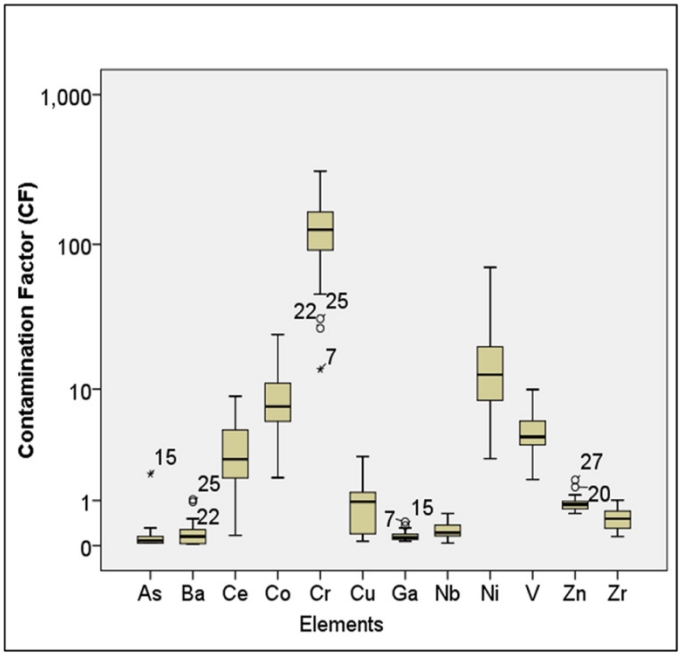
Contamination Factor (CF)
1,000
100
10
1
0
As Ba Ce Co Cr Cu Ga Nb Ni V Zn Zr
Elements

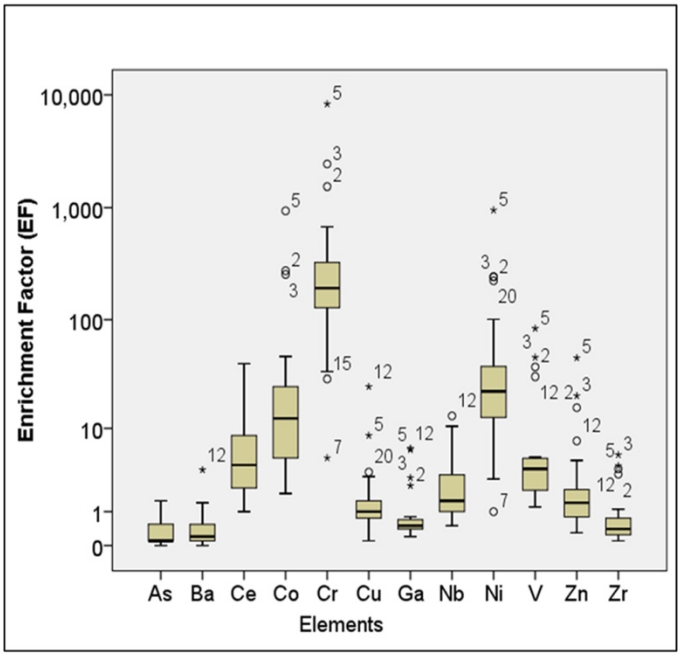
Enrichment Factor (EF)
10,000
1,000
100
10
1
0
As Ba Ce Co Cr Cu Ga Nb Ni V Zn Zr
Elements

FIGURE 5

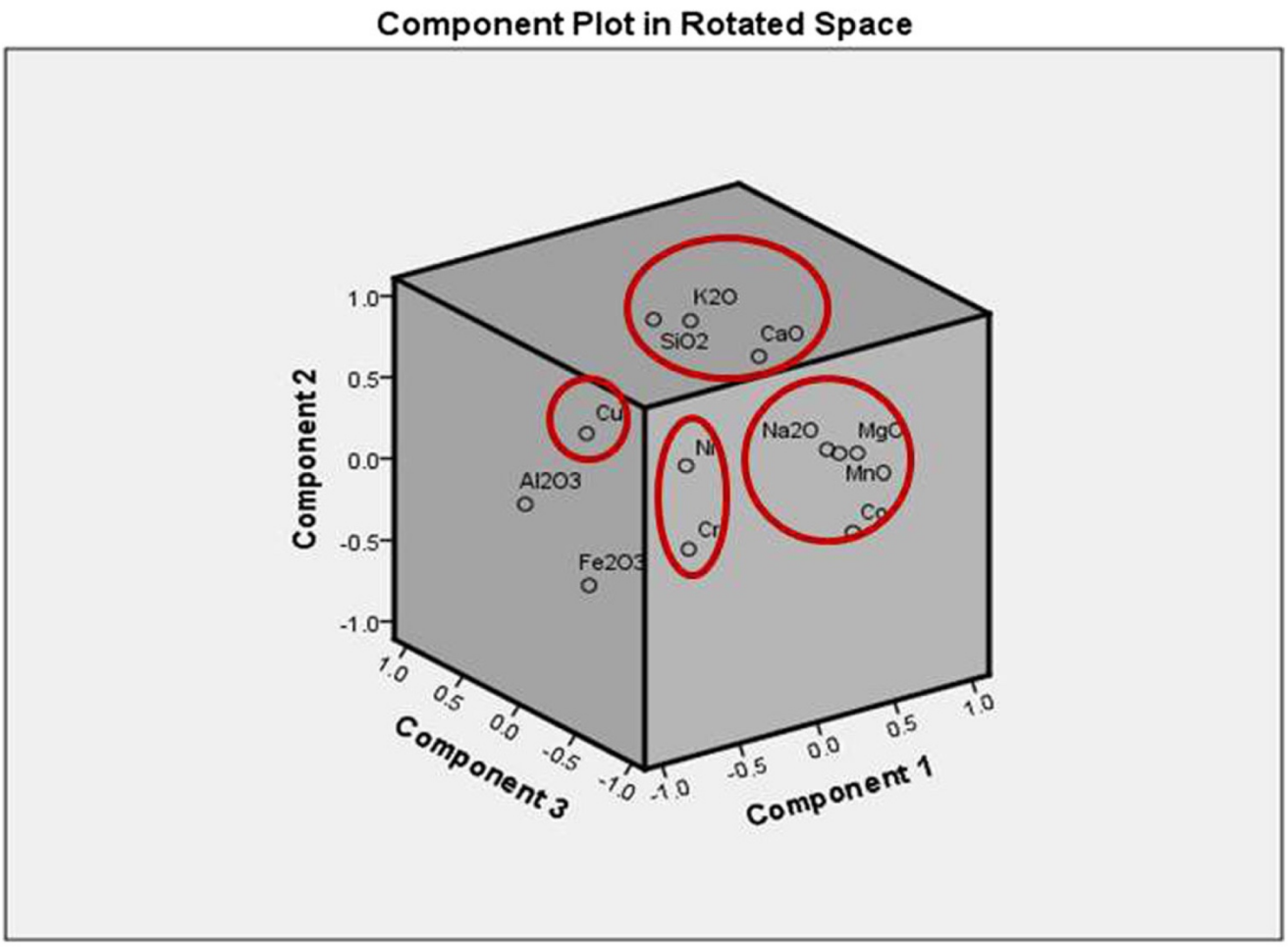
Component Plot in Rotated Space
K2O
SiO2
CaO
Cu
Al2O3
Fe2O3
Na2O
MgO
MnO
Component 2
Component 3
Component 1
1.0
0.5
0.0
-0.5
-1.0

Value	Soil quality	Value	Enrichment level	Value	Contamination factor	Value
Igeo < 0	Practically uncontaminated	EF < 2	Deficiency or minimal enrichment	CF < 1	Low contamination	RI < 150
0 < Igeo < 1	Uncontaminated to moderately contaminated	2 < EF < 5	Moderate enrichment	1 ≤ CF < 3	Moderate contamination	150 ≤ RI < 300
1 < Igeo < 2	Moderately contaminated	5 < EF < 20	Significant enrichment	3 ≤ CF < 6	Considerable contamination	300 ≤ RI < 600
2 < Igeo < 3	Moderately to heavily contaminated	20 < EF < 40	Very high enrichment	6 ≤ CF	Very high contamination	600 ≤ RI
3 < Igeo < 4	Heavily contaminated	EF > 40	Extremely high enrichment			
4 < Igeo < 5	Heavily to extremely contaminated					
5 < Igeo	Extremely contaminated					

TABLE 1

TABLE 2

Parameter	Min-max [mean]	Median ± STD	VC	Skewness	Kurtosis	Upper Continental Crust[a]
pH	5.02–7.22 [5.78]	5.72 ± 0.50	0.25	1.18	2.63	–
CEC ($cmol^{(+)}\ kg^{-1}$)	1.20–33.87 [9.33]	5.41 ± 8.74	76.34	1.64	2.16	–
Particle size distribution (%)						
> 2 mm	<0.001–3.00 [0.50]	0.00 ± 0.83	0.68	1.86	3.44	n.a.
Sand	18.00–67.00 [27.15]	23.50 ± 11.35	128.77	2.44	7.71	n.a.
Silt	25.00–61.00 [51.50]	53.50 ± 9.13	83.32	− 1.78	3.38	n.a.
Clay	<0.001–55.00 [21.15]	19.50 ± 12.17	148.03	0.92	1.86	n.a.
Major oxides (wt%)						
SiO_2	5.17–60.50 [25.11]	21.52 ± 13.13	172.52	1.65	2.75	n.a.
TiO_2	<0.001–2.10 [0.59]	0.50 ± 0.45	0.20	1.50	3.74	n.a.
Al_2O_3	0.20–26.91 [13.30]	12.85 ± 8.10	65.69	− 0.26	− 0.82	n.a.
Fe_2O_3	0.02–55.65 [31.16]	40.91 ± 19.52	381.25	− 0.561	− 1.19	n.a.
MnO	0.08–16.27 [2.59]	0.38 ± 4.88	23.85	1.92	2.25	n.a.
MgO	0.21–65.88 [11.66]	0.76 ± 21.23	450.81	1.73	1.29	n.a.
CaO	0.02–0.36 [0.15]	0.18 ± 0.08	0.01	0.19	0.63	n.a.
Na_2O	<0.001–0.72 [0.13]	0.05 ± 0.19	0.03	2.09	3.57	n.a.
K_2O	<0.001–1.95 [0.25]	0.16 ± 0.42	0.18	3.22	10.90	n.a.
P_2O_5	0.03–0.74 [0.12]	0.06 ± 0.17	0.03	2.68	7.11	n.a.
Trace elements ($mg\ kg^{-1}$)						
As	0.5–26 [2.2]	1 ± 5	24	4.76	23.81	1.5
Ba	10–597 [129]	85 ± 155	24,098	1.95	3.71	550
Ce	10–523 [203]	162 ± 133	17,693	0.78	0.36	64
Co	35–464 [166]	141 ± 92	8512	1.53	3.16	17
Cr	1248–27,900 [11,400]	11,200 ± 5945	35,345,815	0.52	0.94	83
Cu	3–131 [43]	43 ± 33	1093	0.73	0.42	25
Ga	3–20 [7]	6 ± 4	18	1.36	1.95	n.a.
Nb	2–29 [12]	10 ± 7	46	1.05	1.02	12
Ni	189–4753 [1120]	865 ± 883	779,467	2.83	10.84	44
V	120–675 [326]	291 ± 141	19,985	0.98	0.95	107
Zn	61–165 [87]	84 ± 23	528	1.92	4.7	71
Zr	14–96 [48]	48 ± 24	587	0.29	− 1.03	190

TABLE 3

	Kruskal-Wallis *p* value	Mann-Whitney	Result
SiO_2	0.43	0.46	Not different
TiO_2	0.28	0.29	Not different
Al_2O_3	0.17	0.18	Not different
Fe_2O_3	0.85	0.87	Not different
MnO	0.25	0.26	Not different
MgO	0.85	0.86	Not different
CaO	0.00	0.00	Different
Na_2O	0.13	0.14	Not different
K_2O	0.03	0.03	Different
P_2O_5	0.00	0.00	Different
As	0.13	0.14	Not different
Ba	0.96	0.98	Not different
Ce	0.02	0.02	Different
Co	0.01	0.01	Different
Cr	0.01	0.01	Different
Cu	0.01	0.01	Different
Ga	0.46	0.47	Not different
Nb	0.01	0.01	Different
Ni	0.00	0.00	Different
V	0.00	0.00	Different
Zn	0.35	0.37	Not different
Zr	0.01	0.01	Different

TABLE 4

	Al	Ba	Ca	Co	Cr	Cu	Fe	K	Li	Mg	Mn	Na	Ni	Pb	Sr	V	Zn
Peninsular surface water (μg L^{-1})																	
Min	0	3	3800	1	2	2	202	326	5	62,400	14	5200	4	1	22	1	4
Max	1331	121	21,300	3	21	13	1089	2020	28	621,500	359	61,400	24	8	42	4	5
Mean	422	25	10,000	1	9	4	659	776	16	182,000	150	27,900	11	3	31	2	5
Median	258	8	8,800	1	7	2	583	721	14	92,400	98	26,500	6	1	33	2	5
Std.	463	43	5,600	1	7	4	344	580	9	200,900	121	20,500	9	3	7	1	1
Sabah surface water (μg L^{-1})																	
Min	0	4	4,800	1	5	42	359	365	6	84,800	9	26,500	11	1	23	2	20
Max	630	151	11,000	7	14	326	1920	770	37	253,600	220	66,100	94	3	57	5	80
Mean	284	30	8,400	3	8	149	963	575	22	134,900	76	53,400	40	2	43	4	43
Median	269	8	8,900	2	8	129	862	577	23	98,500	60	62,400	33	2	45	4	29
Std.	190	50	2,000	2	3	102	585	193	12	69,500	68	15,700	29	1	13	1	23
Sub-surface water (μg L^{-1})																	
Min	116	7	8,400	4	23	2	68	380	10	122,800	9	15,200	95	1	25	1	4
Max	2301	33	22,800	22	172	1654	3344	2097	33	631,400	459	65,100	936	4	93	3	134
Mean	916	17	13,300	11	91	553	1170	1044	25	297,400	177	47,600	380	3	57	2	48
Median	332	12	8,800	8	77	3	97	654	32	138,100	62	62,600	110	3	54	2	6
Std.	1204	14	8,200	10	75	954	1883	922	13	289,300	246	28,100	481	2	34	1	75
WHO	200	700	–	–	50	2000	–	–	–	–	–	50	70	10	–	–	–
INWQS	50	1000	–	50	50	–	300	–	–	–	–	–	100	50	–	–	5000

TABLE 5

	Co			Cr			Cu			Ni			V		
	Igeo	EF	CF	Igeo	EF	CF	Igeo	EF	CF	Igeo	EF	CF	Igeo	EF	CF
Min	0.3	1.9	1.8	3.2	5.0	13.9	− 4.5	0.1	0.1	0.9	1.0	2.8	− 0.7	1.2	0.9
Max	4.0	936.1	24.4	7.7	8300	310	1.0	24.8	2.9	5.5	951	69.9	1.8	83.4	5.2
Mean	2.3	66.3	8.7	6.1	638	127	− 1.4	2.3	0.9	3.1	81.1	16.5	0.6	10.1	2.5

TABLE 6

	SiO_2	TiO_2	Al_2O_3	Fe_2O_3	MnO	MgO	CaO	Na_2O	K_2O	Co	Cr	Cu	Ni	V	Zn
SiO_2	1														
TiO_2	0.17	1													
Al_2O_3	−0.12	0.87**	1												
Fe_2O_3	−0.26	0.16	0.38	1											
MnO	−0.53**	−0.50**	−0.37*	−0.18	1										
MgO	−0.15	−0.63**	−0.66**	−0.51**	.56**	1									
CaO	0.59**	−0.16	−0.32	−0.08	−0.2	0.07	1								
Na_2O	0.15	−0.42*	−0.53**	−0.36	0.15	.54**	.47*	1							
K_2O	.53**	−0.1	−0.32	−0.09	−0.16	0.08	.73**	.48*	1						
Co	−0.34	−0.52**	−0.41*	0.18	.48*	0.311	0.29	0.21	0.14	1					
Cr	−0.71**	−0.12	0.09	0.13	0.27	0.2	−0.55**	−0.18	−0.67**	0.25	1				
Cu	0.01	0.57**	0.55**	−0.26	−0.13	−0.17	−0.48*	−0.23	−0.39*	−0.70**	0.12	1			
Ni	−0.31	−0.28	−0.09	−0.06	0.03	0.44*	−0.35	0.03	−0.42*	0.05	.69**	0.07	1		
V	−0.1	0.37	0.28	−0.08	0.19	−0.36	0.09	−0.02	0.03	0.1	−0.27	0.11	−0.74**	1	
Zn	−0.28	−0.51**	−0.41*	−0.2	0.36	0.60**	−0.14	0.38*	−0.04	0.42*	0.49**	−0.12	0.63**	−0.39*	1

TABLE 7

	Component			
	F1	F2	F3	F4
SiO_2	−0.105	*0.922*	0.194	−0.150
Al_2O_3	− *0.788*	−0.104	0.394	−0.004
Fe_2O_3	− *0.833*	−0.365	−0.236	0.070
MnO	*0.951*	−0.107	−0.002	−0.113
MgO	*0.972*	−0.065	−0.132	0.029
CaO	0.180	*0.816*	−0.350	−0.180
Na_2O	*0.792*	−0.003	−0.112	−0.005
K_2O	0.020	*0.939*	0.037	0.046
Co	0.520	−0.219	− *0.717*	0.158
Cr	−0.035	−0.429	−0.021	*0.810*
Cu	0.018	−0.086	*0.957*	0.044
Ni	−0.042	0.078	−0.007	*0.918*